Article Subject (see Index Terms below and write one here) _____

Frequency-Coded and Programmable Synchronous Electromagnetic Encoders Based on Linear Strips

Amirhossein Karami-Horestani, Ferran Paredes, and Ferran Martín*

CIMITEC, Departament d'Enginyeria Electrònica, Universitat Autònoma de Barcelona, 08193 Bellaterra, Spain
* Fellow, IEEE

Abstract—This paper presents electromagnetic encoders where encoding is achieved by considering four different inclusions, particularly linear strips of different length, etched at the predefined positions of the encoder chain, and transversely oriented with regard to the chain axis. Since the length of the strips determines their resonance frequencies, it follows that the 2-bits per inclusion, corresponding to the four possible different states (strip lengths), are frequency-coded. Thus, the reader is a microstrip line with a series gap fed by four harmonic (carrier) signals tuned to the resonance frequencies of the four considered encoder strips. By encoder motion over the reader, each carrier signal is amplitude modulated (AM), with envelope functions exhibiting a peak each time a strip of the encoder chain tuned to the resonance frequency of the considered carrier signal crosses the axis of the reader line. The functionality of the system is experimentally validated in this paper. It is also shown that the encoders can be programmed by considering identical strips and by cutting them appropriately, according to the desired code. The proposed encoders are intrinsically synchronous. Such encoders are useful for measuring displacements and velocities, as well as for the implementation of synchronous near-field chipless radiofrequency identification (chipless-RFID) tags with sequential bit reading.

Index Terms—Displacement sensors, electromagnetic encoders, microstrip technology, motion control.

I. INTRODUCTION

Electromagnetic encoders are an alternative to optical [1]-[3] and magnetic encoders [4]-[6]. The main advantage of electromagnetic encoders as compared to optical encoders is their superior robustness against the presence of dirtiness, grease, or pollution, present in many industrial environments. As compared to magnetic encoders, that typically need inductive coils, or to Hall effect sensors [7]-[12], based on magnets, electromagnetic encoders are relatively simple and low-cost, as far as electromagnetic encoders are based on a movable element consisting in a low-cost dielectric material with printed (typically metallic) inclusions, and the stator (or reader) is a transmission line structure conveniently feed by a harmonic signal, or a set of harmonic signals.

Both rotary [13]-[14] and linear [15]-[21] electromagnetic encoders have been presented. Moreover, it has been shown that linear electromagnetic encoders can be applied not only in motion control systems (as linear displacement/velocity sensors), but also for the implementation of near-field chipless radiofrequency identification (chipless-RFID) systems with sequential bit reading [15]-[17],[21]-[23]. A key performance parameter in electromagnetic encoders for both applications (displacement/velocity sensor and near-field chipless-RFID) is the per-unit-length density of bits. This provides the spatial resolution in displacement sensors and the data capacity that can be accommodated in a certain encoder length in chipless-RFID tags.

Another important aspect in electromagnetic encoders is synchronous reading. This typically requires at least two encoder chains, one of them with all the inclusions present at their predefined positions, providing the clock signal (as well as the encoder velocity), and the other one providing the identification (ID) code [19],[20]. In the latter case, only a subset of functional inclusions is present at the predefined positions, in accordance to the specific ID code. Synchronous reading might be important in chipless-RFID systems, in situations where the encoder velocity over the reader is not precisely known (for example, if the tags are read manually). On the other hand, in displacement and velocity sensors, quasi-absolute measurements can be made by assigning a specific ID code to the whole encoder. If such complete ID code follows the so-called de Bruijn sequence [24], any subset of N adjacent bits does not repeat and each encoder position has a unique ID code, determined by the corresponding bit plus the $N-1$ preceding bits. The number of bits of the subset, N, must satisfy

$$N > \log_2 \frac{L}{p} \qquad (1)$$

where L is the total length of the encoder and p is the period, or position resolution. These electromagnetic encoders equipped with the de Bruijn sequence are designated as quasi-absolute in the sense that the encoder must displace N periods after a system reset in order to determine the absolute position. This represents a slight disadvantage as compared to the so-called absolute (optical) encoders (where such "initial" displacement is not needed), but quasi-absolute encoders are not based on accumulative pulse counting, such as

incremental encoders (i.e., those not equipped with an ID code) do [13].

In this paper, we report a proof-of-concept of a synchronous electromagnetic encoder based on a single chain of inclusions, particularly linear metallic strips transversally oriented with regard to the chain axis. An inclusion is always present at the predefined position of the chain, and this provides synchronism to the system. However, the length of the inclusions may vary between four different values, corresponding to four different states and, consequently, to two bits of information per inclusion. By this means, the density of bits per unit length is twice the one of those tags simply based on absence/presence of functional inclusions at the predefined positions, where synchronism requires typically an additional (clock) chain [19],[20].

II. THE PROPOSED ENCODER SYSTEM AND WORKING PRINCIPLE

Figure 1(b) depicts a typical encoder, consisting in a chain of transversally oriented metallic strips (inclusions) of different length. In this work, four different strip lengths are considered, corresponding to two bits per inclusion. For encoder reading, an element able to detect the different lengths of the strips is necessary. This can be achieved by means of a transmission line with a series gap (Fig. 1a). Such gap prevents signal transmission between the input and the output port. However, when a strip is on top of the line, and aligned with the line axis, such strip behaves similar to a half wavelength resonator, and a peak in the frequency response arises. Thus, by simultaneously feeding the line with four harmonic signals tuned to the resonance frequencies of the different strips, the specific strip length, when the encoder is displaced over the reader at short distance, can be detected. For each (carrier) frequency, one expects that the amplitude is modulated by encoder motion. Specifically, the amplitude of a certain carrier signal is expected to be high when the strip tuned to that frequency is on top of the line axis. Thus, by recording the envelope function of each carrier signal at the output port, the complete ID code of the encoder can be retrieved.
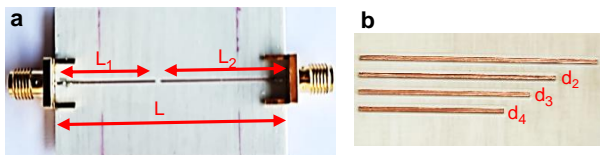

Fig. 1. (a) photograph of the fabricated transmission line reader, with a series gap. The width of the transmission line is 0.4 mm and other dimensions are $L_1 = 22$ mm, $L_2 = 27$ mm, and $L = 50$ mm. (b) photograph of a typical (8-bit) encoder. The period of the encoder is $p = 2$ mm and strip width is 0.5 mm. The lengths of the 4 encoder strips are $d_1 = 28$ mm, $d_2 = 24$ mm, $d_3 = 20$ mm, $d_4 = 16$ mm. The considered substrate of the encoder and reader is the *Rogers 4003C* with thickness $h = 0.81$ mm, dielectric constant $\varepsilon_r = 3.55$ and loss tangent $\tan\delta = 0.0022$.

In a real scenario, an input combiner can be used to feed the reader line with the four harmonic signals, and an output multiplexer can be used for the separation of the different AM signals. In this case, four envelope detectors are needed. A preferred option, the one considered

in the sketch of Fig. 2, considers a voltage controlled oscillator (VCO) managed by a microcontroller, so that the frequency of the single injected signal varies periodically between the four required values (resonance frequencies of the linear strips). The AM signals are separated at the output port also by means of the microcontroller, and thus the four envelope functions can be inferred. With this approach, a single envelope detector is needed.

In order to reduce the encoder period as much as possible, it is convenient to achieve as much peaked frequency responses as possible, when the strips are on top of the line axis. This aspect is intimately related to the loaded quality factor of the strip resonators, which depends on the width of the strip, on the air gap, or vertical distance between the reader line and the encoder chain (it is assumed in this work that the strips of the encoder are oriented face-to-face with the reader line), and also on the dielectric and metal losses. The estimated loaded quality factor is of the order of 13, 18, 17, and 19 for the four resonators from the longest to the shortest, respectively. Nevertheless, the presence of adjacent strips, as actually occurs in the encoder, may play a role, especially if the period is small.

Thus, to analyze the influence of the air gap and strip width, we have first carried out electromagnetic simulations (by means of the *Ansys HFSS* electromagnetic solver) of the transmission coefficient for each carrier frequency as a function of the displacement for the considered 8-bit encoder of Fig. 1(b), considering the air gap as a parameter. Note that the period of such encoder is $p = 2$ mm, corresponding to a per-unit-length bit density of 10 bit/cm, a competitive value for a synchronous encoder. The results are depicted in Fig. 3. It can be seen that for air gaps of 0.5 mm, 1.0 mm and 1.5 mm, the capacity of discrimination of the proposed system is very reasonable. Particularly, it can be appreciated that when a certain strip resonator is on top of the line axis, at the frequency of such resonator the transmission is high, whereas at the other frequencies, it decreases significantly, and this occurs for the four strip resonators. Nevertheless, for an extremely small air gap of 0.2 mm, this discrimination capability is limited. Thus, it is convenient to set the air gap separation at least to 0.5 mm.

In a second set of simulations, we have set the air gap to 0.5 mm, and we have obtained the transmission coefficient for each carrier frequency as a function of the displacement for the considered 8-bit encoder of Fig. 1(b), parametrized by the width of the strips. However, the results are roughly undistinguishable from those of Fig. 3(b), with
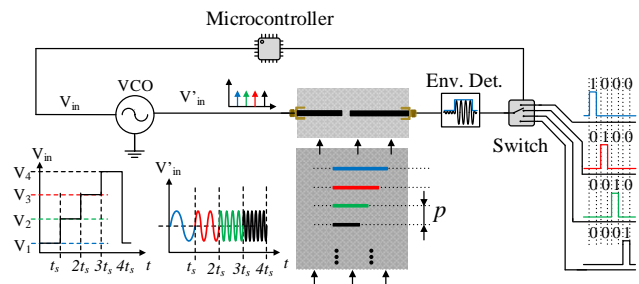

Fig. 2. Sketch showing the working principle of the proposed frequency-coded encoder system with synchronous reading. The sketch of the synchronous system based on a double chain of inclusions can be found in [20].
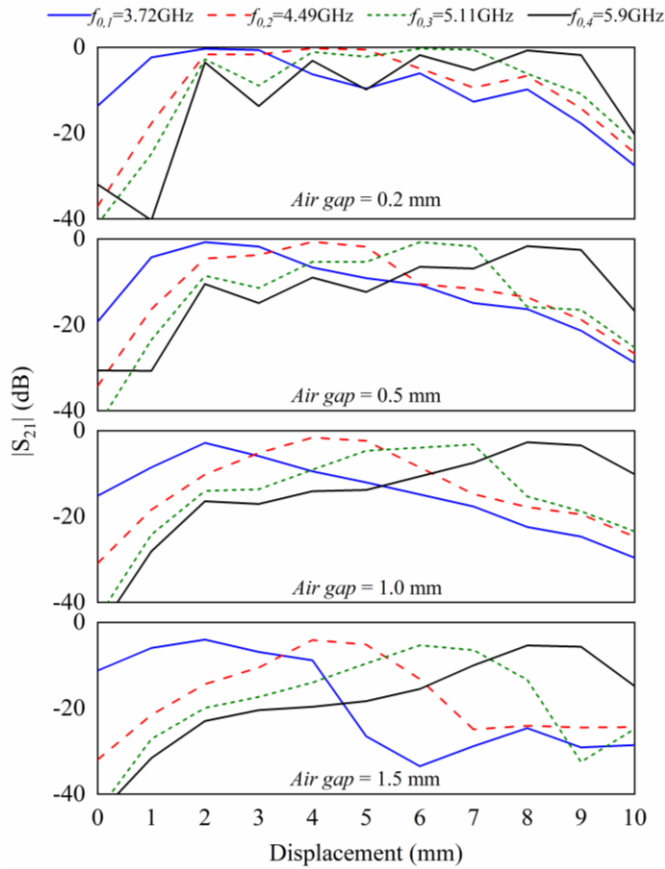
Fig. 3. Simulation of the transmission coefficient for the resonance frequencies of the four strip resonators of the encoder, as a function of the encoder displacement, considering the air gap as a parameter. (a) air gap 0.2 mm; (b) air gap 0.5 mm; (c) air gap 1.0 mm; (d) air gap 1.5 mm. The considered encoder is depicted in Fig. 1, with a period set to $p = 2$ mm, and strip width set to 0.5 mm.

a strip width set to 0.5 mm, the nominal value of the encoders of this work (hence these simulations are not depicted). This means that, at least for the considered air gap separation (0.5 mm, the nominal one), the strip width does not have a significant influence.

III. EXPERIMENTAL RESULTS

For experimental validation, rather than the 8-bit encoder of Fig. 1(b), we have fabricated a 40-bit encoder consisting in a chain of 20 identical strip resonators (the length of such strips is the longest one). Then, we have made cuts on different resonant strips, thereby generating new ID codes by programming the encoders. Obviously, the cuts are made in positions that provide new strip resonators of one of the considered lengths. The tag before cutting and those that result after each step of cutting are shown in Figure 4. Figure 5 depicts the envelope functions of the different generated 40-bit encoders. There is a perfect correlation between the responses (envelope functions) and the strips of the different encoders. Consequently, with these results, the functionality of the system is experimentally validated.
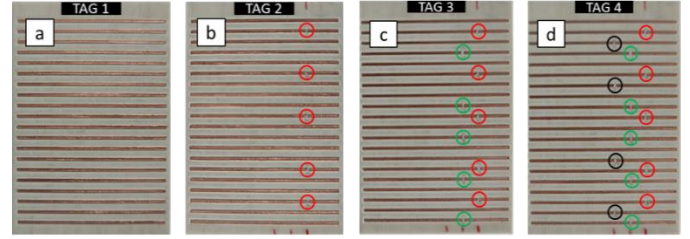

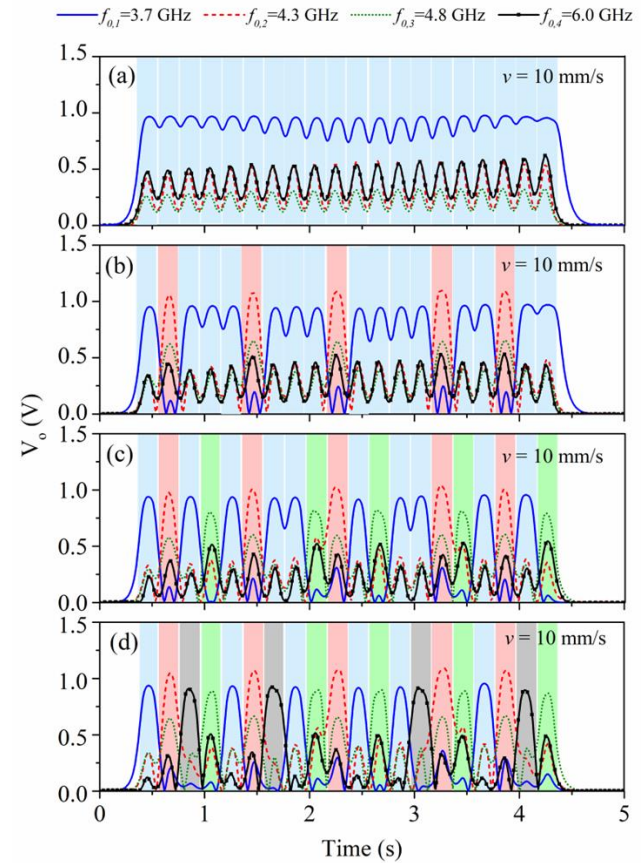Fig. 4. The tag before cutting and after each step of cutting

Fig. 5. Measured envelope functions for the four frequencies corresponding to the resonances of the four strip resonators, for the encoders depicted in Fig. 4. (a) Envelope function corresponding to TAG 1, (b) envelope function to TAG 2, (c) envelope function to TAG 3, (d) envelope function corresponding to TAG 4. Air gap = 0.5 mm.

IV. COMPARISON TO OTHER ENCODERS

There are several synchronous electromagnetic encoders available in the literature [17],[19]-[21] (see Table 1). As compared to such encoders, the encoder proposed in this paper is the one exhibiting the higher density of bits per unit length (DPL) and per surface area (DPS). Certainly, there are other electromagnetic encoders exhibiting a superior value of the DPL [15],[25], but such encoders are not synchronous. In fact, the synchronous encoders of the present work exhibit also a very competitive DPS because the clock signal is not necessary. The reason is that a strip inclusion is always present at the predefined positions of the encoder chain. Therefore, a single encoder chain (containing the ID code) suffices, and this represents a competitive advantage in terms of encoder size and DPS.

Table 1. Comparison of various electromagnetic encoders.

Ref.	Sync.	Direction detection	DPS (bits/cm²)	DPL (bits/cm)
[17]	Yes	No	1.15	1.67
[19]	Yes	Yes	1.63	6.96
[20]	Yes	Yes	0.8	2.4
[21]	Yes	No	0.89	2.5
[15]	No	No	26.0	16.7
[25]	No	No	4.90	16.7
This work	**Yes**	**No**	**3.34**	**10**

Let us also mention that significant values of the DPS have been demonstrated in certain encoders based on the frequency domain, although not read sequentially [26],[27].

V. CONCLUSION

In conclusion, a new type of electromagnetic encoders providing synchronous reading with a single inclusions' chain and a per-unit length data density of DPL = 10 bit/cm has been experimentally demonstrated. Such high data density has been achieved by virtue of the small encoder period (related to the use of narrow linear strips), and thanks to frequency encoding of the inclusions, a strategy that doubles the number of bits per inclusion.

ACKNOWLEDGMENT

REFERENCES

[1] E. Eitel, "Basics Of Rotary Encoders: Overview and New Technologies," *Machine Design Magazine*, vol. 4, no. 2, 2015.

[2] G. K. McMillan and D. M. Considine, "Process/Industrial Instrument and Control Handbook," in *Symposium A Quarterly Journal In Modern Foreign Literatures*, 1999.

[3] X. Li, J. Qi, Q. Zhang, and Y. Zhang, "Bias-tunable dual-mode ultraviolet photodetectors for photoelectric tachometer," *Applied Physics Letters*, vol. 104, no. 4, 2014, doi: 10.1063/1.4863431.

[4] Z. Zhang, Y. Dong, F. Ni, M. Jin, and H. Liu, "A Method for Measurement of Absolute Angular Position and Application in a Novel Electromagnetic Encoder System," *Journal of Sensors*, vol. 2015, 2015, doi: 10.1155/2015/503852.

[5] K. Nakano, T. Takahashi, and S. Kawahito, "A CMOS smart rotary encoder using magnetic sensor arrays," in Proceedings of the 2nd International Conference on Sensors (Sensors '03), vol. 1, pp. 206–209, IEEE, October 2003.

[6] Z. Zhang, F. Ni, Y. Dong, M. Jin, and H. Liu, "A novel absolute angular position sensor based on electromagnetism," *Sensors and Actuators, A: Physical*, vol. 194, 2013, doi: 10.1016/j.sna.2013.01.040.

[7] J. Jezný and M. Čurilla, "Position Measurement with Hall Effect Sensors," *American Journal of Mechanical Engineering*, vol. 1, no. 7, 2013.

[8] P. N. Granell *et al.*, "Highly compliant planar Hall effect sensor with sub 200 nT sensitivity," *npj Flexible Electronics*, vol. 3, no. 1, 2019, doi: 10.1038/s41528-018-0046-9.

[9] A. Lidozzi, L. Solero, F. Crescimbini, and A. di Napoli, "SVM PMSM drive with low resolution hall-effect sensors," *IEEE Transactions on Power Electronics*, vol. 22, no. 1, 2007, doi: 10.1109/TPEL.2006.886603.

[10] G. Scelba, G. de Donato, G. Scarcella, F. Giulii Capponi, and F. Bonaccorso, "Fault-tolerant rotor position and velocity estimation using binary hall-effect sensors for low-cost vector control drives," *IEEE Transactions on Industry Applications*, vol. 50, no. 5, 2014, doi: 10.1109/TIA.2014.2304616.

[11] X. Zhang, M. Mehrtash, and M. B. Khamesee, "Dual-axial motion control of a magnetic levitation system using Hall-effect sensors," *IEEE/ASME Transactions on Mechatronics*, vol. 21, no. 2, 2016, doi: 10.1109/TMECH.2015.2479404.

[12] G. Liu, B. Chen, and X. Song, "High-Precision Speed and Position Estimation Based on Hall Vector Frequency Tracking for PMSM with Bipolar Hall-Effect Sensors," *IEEE Sensors Journal*, vol. 19, no. 6, 2019, doi: 10.1109/JSEN.2018.2885020.

[13] J. Mata-Contreras, C. Herrojo, and F. Martin, "Application of Split Ring Resonator (SRR) Loaded Transmission Lines to the Design of Angular Displacement and Velocity Sensors for Space Applications," *IEEE Transactions on Microwave Theory and Techniques*, vol. 65, no. 11, 2017, doi: 10.1109/TMTT.2017.2693981.

[14] C. Herrojo, J. Mata-Contreras, F. Paredes, and F. Martín, "Microwave Encoders for Chipless RFID and Angular Velocity Sensors Based on S-Shaped Split Ring Resonators," *IEEE Sensors Journal*, vol. 17, no. 15, 2017, doi: 10.1109/JSEN.2017.2715982.

[15] C. Herrojo, F. Paredes, and F. Martin, "Double-Stub Loaded Microstrip Line Reader for Very High Data Density Microwave Encoders," *IEEE Transactions on Microwave Theory and Techniques*, vol. 67, no. 9, 2019, doi: 10.1109/tmtt.2019.2929128.

[16] C. Herrojo, F. Paredes, J. Bonache, and F. Martin, "3-D-Printed High Data-Density Electromagnetic Encoders Based on Permittivity Contrast for Motion Control and Chipless-RFID," *IEEE Transactions on Microwave Theory and Techniques*, vol. 68, no. 5, 2020, doi: 10.1109/TMTT.2019.2963176.

[17] F. Paredes, C. Herrojo, R. Escude, E. Ramon, and F. Martin, "High Data Density Near-Field Chipless-RFID Tags with Synchronous Reading," *IEEE Journal of Radio Frequency Identification*, vol. 4, no. 4, 2020, doi: 10.1109/JRFID.2020.2996586.

[18] F. Paredes, C. Herrojo, and F. Martin, "Microwave encoders with synchronous reading and direction detection for motion control applications," in *IEEE MTT-S International Microwave Symposium Digest*, 2020, vol. 2020-August. doi: 10.1109/IMS30576.2020.9224044.

[19] C. Herrojo, F. Paredes, and F. Martin, "Synchronism and Direction Detection in High-Resolution/High-Density Electromagnetic Encoders," *IEEE Sensors Journal*, vol. 21, no. 3, 2021, doi: 10.1109/JSEN.2020.3025435.

[20] F. Paredes *et al.*, "Electromagnetic Encoders Screen-Printed on Rubber Belts for Absolute Measurement of Position and Velocity," *Sensors*, vol. 22, no. 5, 2022, doi: 10.3390/s22052044.

[21] A. Karami-Horestani, F. Paredes and F. Martín, "A Hybrid Time/Frequency Domain Near-Field Chipless-RFID system", 21st Mediterranean Microwave Symposium, Pizzo Calabro, Italy, May 9-13, 2022.

[22] C. Herrojo, J. Mata-Contreras, A. Nunez, F. Paredes, E. Ramon, and F. Martin, "Near-Field Chipless-RFID System with High Data Capacity for Security and Authentication Applications," *IEEE Transactions on Microwave Theory and Techniques*, vol. 65, no. 12, 2017, doi: 10.1109/TMTT.2017.2768029.

[23] C. Herrojo, J. Mata-Contreras, F. Paredes, A. Nunez, E. Ramon, and F. Martin, "Near-Field Chipless-RFID System with Erasable/Programmable 40-bit Tags Inkjet Printed on Paper Substrates," *IEEE Microwave and Wireless Components Letters*, vol. 28, no. 3, 2018, doi: 10.1109/LMWC.2018.2802718.

[24] N. G. de Bruijn, "Acknowledgement of Priority to C. Flye Sainte-Marie on the counting of circular arrangements of 2n zeros and ones that show each n-letter word exactly once," *T.H.-Report 75-WSK-06, Technological University Eindhoven.*, 1975.

[25] J. Havlicek, C. Herrojo, F. Paredes, J. Mata-Contreras, and F. Martin, "Enhancing the Per-Unit-Length Data Density in Near-Field Chipless-RFID Systems with Sequential Bit Reading," *IEEE Antennas and Wireless Propagation Letters*, vol. 18, no. 1, 2019, doi: 10.1109/LAWP.2018.2881356.

[26] R. Rezaiesarlak and M. Manteghi, "Complex-natural-resonancebased design of chipless RFID tag for high-density data," *IEEE Trans. Antennas Propag.*, vol. 62, no. 2, pp. 898–904, Feb. 2014.

[27] M. A. Islam, N. C. Karmakar, "A novel compact printable dual-polarized chipless RFID system," *IEEE Trans. Microw. Theory Techn.*, vol. 60, pp. 2142–2151, 2012.